

Role of host excimer formation in the degradation of organic light-emitting devices

Robert Newcomb^{a,‡}, John S. Bangsund^{a,‡}, Kyle W. Hershey^{a,†}, Dominea C. K. Rathwell^b, Hong-Yeop Na^b, Jeong-Hwan Jeon^b, Peter Trefonas^c, Russell J. Holmes^{a,*}

^aDepartment of Chemical Engineering and Materials Science, University of Minnesota, Minneapolis, MN, 55455, USA

^bDuPont Korea Technology Center, Hwaseong, Gyeonggi-Do, 18449, Korea

^cDuPont Electronics and Imaging, Marlborough, MA, 01752 USA

[‡]These authors contributed equally [†]Present address: Microsoft Corporation, Redmond, WA, 98052, USA ^{*}Corresponding author: rholmes@umn.edu

Abstract

Host-guest structures are used in most state-of-the-art organic light-emitting devices (OLEDs), with the host transporting charge and confining excitons on the guest. While the host often plays a critical role in achieving high efficiency and stability, predicting and understanding these effects is a persistent design challenge which slows the discovery of new active materials. Closely related host molecules, which differ only by several functional groups, often show drastically different degradation behavior. Here, we explore this observation for the archetypical carbazole hosts 4'-bis(N-carbazolyl)-1,1'-biphenyl (CBP) and 4,4'-bis(carbazole-9-yl)-2,2'-dimethylbiphenyl (CDBP). While devices based on these hosts show similar efficiencies, CDBP-based devices show a tenfold lower lifetime than CBP devices when paired with phosphorescent or fluorescent emitters. Using optically- and electrically-pumped degradation tests, mass spectrometry, compositional analysis and low-temperature phosphorescence spectroscopy, the lifetimes of devices containing CDBP are shown to correlate with the formation of intermolecular triplet excimer states. These findings suggest that candidate host molecules should be screened for excimer formation, as host excimers may aggravate device degradation and lower device stability.

This is the author's peer reviewed, accepted manuscript. However, the online version of record will be different from this version once it has been copyedited and typeset.

PLEASE CITE THIS ARTICLE AS DOI: 10.1063/1.5124802

Organic light-emitting devices (OLEDs) have become an established display technology, finding especially broad commercialization for mobile applications.¹⁻³ Despite this, further adoption of OLEDs could be realized with additional improvements in molecular and device design for long operational lifetime. The OLED emissive layer (EML) frequently contains two molecular systems, mixing a highly luminescent guest at low concentration with a host that serves to space guest molecules to maximize luminescence efficiency, and may also serve to transport charge and excitons.^{1,4,5} Host selection is often made based on the electronic and excitonic energy levels in order to maximize exciton confinement on the guest.^{6,7} This has led to a wide range of host materials being realized via chemical functionalization with a range of singlet and triplet energies.^{5,8,9} While improved exciton confinement frequently leads to enhanced device efficiencies, trends in degradation are often not as clear.⁹⁻¹¹ Indeed, seemingly small changes in host molecular structure can lead to significant changes in device stability, likely reflecting changes in nanoscale packing, morphology, and/or intermolecular interactions.^{9,12-15}

Among the most widely studied hosts are those containing carbazole moieties, which have been widely implemented in phosphorescent OLEDs and OLEDs based on thermally activated delayed fluorescence (TADF).⁸ Carbazoles perform well as host materials due to their typically ambipolar charge transport properties and high triplet energies, which ensure effective guest exciton confinement.⁸ Two archetypal carbazole hosts are 4,4'-bis(N-carbazolyl)-1,1'-biphenyl (CBP)^{16,17} and 4,4'-bis(carbazole-9-yl)-2,2'-dimethylbiphenyl (CDBP).⁶ These similarly structured hosts, which differ by only two methyl groups, show a stark contrast in device stability. Here, we consider the degradation of OLEDs based on the archetypal green phosphorescent emitter tris[2-phenylpyridinato-C2,N]iridium(III) (Ir(ppy)₃) paired with each host. We find that the reduced lifetime of devices based on CDBP is related to the tendency of CDBP to form triplet

This is the author's peer reviewed, accepted manuscript. However, the online version of record will be different from this version once it has been copyedited and typeset.

PLEASE CITE THIS ARTICLE AS DOI: 10.1063/1.5124802

excimers. Since carbazole hosts are often susceptible to excimer formation,^{9,18} these findings could inform molecular screening criteria for developing more stable host materials.

Devices were constructed on pre-patterned indium-tin-oxide (ITO)-coated glass substrates (Xin Yan). Substrates were cleaned by sequentially sonicating in tergitol, distilled water, and acetone, followed by rinsing in boiling isopropanol. Substrates were treated with UV-ozone ambient for 15 minutes before a planarizing hole-injection layer of Plexcore AQ1250 (Sigma Aldrich) was spun-cast in a N₂ glovebox and annealed for 30 minutes at 150 °C. The remaining organic and metal layers were deposited by high vacuum thermal evaporation at a rate of 0.1 – 0.3 nm/s: a 40-nm-thick hole-transport layer (HTL) of tris(4-carbazoyl-9-ylphenyl) amine (TCTA), followed by a 10-nm-thick EML composed of the host and 7 vol. % Ir(ppy)₃, and a 40-nm-thick electron-transport layer (ETL) of 2,2',2''-(1,3,5-benzinetriyl)-tris(1-phenyl-1-H-benzimidazole) (TPBi). Finally, the cathode consists of 0.5 nm of LiF followed by 100 nm of Al, shadow-masked to define a device area of 0.25 cm². Devices for optical degradation (Figure 3) used a 20-nm-thick EML, with an emitter of either Ir(ppy)₃ or 2,3,6,7-tetrahydro-1,1,7,7-tetramethyl-1H,5H,11H-10-(2-benzothiazolyl) quinolizino-[9,9a,1gh] coumarin (C545T) and an otherwise identical architecture. Devices were encapsulated in an N₂ glovebox with a glass cover slide and UV cured epoxy. Measurements of device external quantum efficiency (EQE) were performed using a Hamamatsu S3584-08 calibrated photodiode and an Agilent 4155C parameter analyzer, assuming Lambertian emission for luminance calculations. Emission spectra were collected with a Princeton Instruments FERGIE spectrometer. Low temperature measurements of film phosphorescence were carried out in a Janis CSS-150 Optical Cryostat at 10 K, using a N₂ laser with a wavelength of $\lambda=337$ nm (repetition rate of 0.5 Hz) to pump the sample. The spectrometer was triggered to measure phosphorescence 5 ms after each laser pulse with an integration window of 1,000 ms.

This is the author's peer reviewed, accepted manuscript. However, the online version of record will be different from this version once it has been copyedited and typeset.

PLEASE CITE THIS ARTICLE AS DOI: 10.1063/1.5124802

Each spectrum was averaged over ~100 pulses. The spectrometer exposure is synchronized with the laser using a Hewlett Packard 8114A pulse generator. Laser Desorption Ionization Time-of-Flight Mass Spectrometry (LDI-TOF-MS) was performed using an Applied Biosystems-Sciex 5800 MALDI-TOF/TOF on degraded and undegraded devices.¹⁹⁻²² Devices were degraded to 10% of initial luminescence to improve fragment signal. Full details regarding sample preparation and measurement procedure for LDI-TOF-MS can be found in the Supplementary Material (SM).

The device architecture used here and the molecular structures of CBP and CDBP are shown in Fig. 1. To characterize the stability for devices based on each host, simultaneous measurements of degradation in device EL and photoluminescence (PL) were made as a function of initial luminance. Recent work has shown simultaneous characterization of EL and PL degradation can be used to quantify losses in the efficiencies of exciton formation and recombination.²³⁻²⁶ Here, PL measurements were taken every 10 minutes during a lifetime test by turning off current and illuminating the device with a $\lambda = 405$ nm laser which selectively pumps the emitter. A low laser power is used (<5 mW/cm²) to ensure photo-induced degradation is negligible, and a thin emissive layer (10 nm) minimizes spatial mismatch between the optical and electrical excitation profiles.²³ With these considerations, measured reductions in PL intensity accurately reflect losses in emitter PL efficiency resulting from EL degradation. Fig. 1d shows the dependence of the EL and PL lifetimes on initial luminance (L_0). The t_{50} lifetime is defined as the time required for a device to degrade to 50% of the starting EL intensity under constant current density. Similarly, t_{80} refers to the time required for the photoluminescence (PL) to reach 80% of the initial intensity. It is evident from Fig. 1d that devices based on CDBP decay as much as 10 times faster than those using CBP under similar degradation conditions. However, the same power-law behavior with similar acceleration factors ($n \approx 1.5$, where n is the exponent in $t_{50} \propto L_0^{-n}$) was

This is the author's peer reviewed, accepted manuscript. However, the online version of record will be different from this version once it has been copyedited and typeset.

PLEASE CITE THIS ARTICLE AS DOI: 10.1063/1.5124802

observed for both hosts. This suggests that while degradation is accelerated in the CDBP case, similar kinetic pathways are likely responsible for the reduction in lifetime.^{23,25,27}

To examine potential differences in intrinsic molecular stability for each host, bond dissociation energy (BDE) calculations were performed using B3LYP, basis set (6-31G*), using Gaussian 16 software. BDEs were calculated for ground state configurations (summarized in the SM), while dihedral C-C bond angle calculations were performed in ground and excited states.^{28–30} The C-N bond was found to be weakest in both hosts, in agreement with previous results.^{30,31} The C-N BDE is almost identical in both hosts (81.75 kcal/mol for CBP and 81.28 kcal/mol for CDBP),^{30,31} while the central C-C bond energy was slightly higher for CBP (112.5 kcal/mol for CBP and 107.7 kcal/mol for CDBP). As typically the weakest bond determines molecular stability,³¹ these results suggest that CDBP is not intrinsically less stable than CBP from a chemical perspective. To confirm these calculations, we investigated of molecular fragmentation *via* LDI-TOF-MS. Prior application of this technique to OLEDs has allowed more detailed investigations of degradation pathways.^{21,22,30,32,33} Here, results from LDI-TOF-MS on degraded devices are consistent with BDE calculations and previous reports,³⁰ with the most abundant fragments forming by cleavage of the weak C-N bond in both CBP and CDBP. Primary results are summarized in Fig. 2. Fragmentation in the two hosts differs only subtly: CBP shows slightly higher formation of fragments cleaved at the C-C bonds (Fig. 2a,c), and the ratio of C-N cleaved fragment peak to the pristine molecule peak in CDBP is higher than for CBP (Fig. 2b,d). These differences may reflect the excited state localization in each host, where the CDBP excited state resides on the carbazole group (possibly accelerating C-N bond scission) and the CBP excited state resides primarily on the biphenyl, near the central C-C bond.¹⁵ Overall, these results confirm that both CDBP and CBP degrade primarily *via* cleavage of C-N bonds.

This is the author's peer reviewed, accepted manuscript. However, the online version of record will be different from this version once it has been copyedited and typeset.

PLEASE CITE THIS ARTICLE AS DOI: 10.1063/1.5124802

Taken together, the results of Figs. 1 and 2 suggest that CBP and CDBP share a common primary degradation mechanism. In devices containing CDBP however, these same processes are accelerated. A notable difference between these hosts is that CDBP forms a triplet excimer state, while CBP does not.^{9,15,18} In other words, the first excited triplet state in CDBP is delocalized across adjacent molecules, while that of CBP is a localized triplet residing on a single molecule. Bagnich *et al.* have argued that excimer formation is caused by rotation of the center C-C bond in CDBP, which decreases coupling between the end carbazole groups, moves the excited state to the ends of the molecule, and consequently allows greater orbital overlap between neighboring carbazole groups, where the excimer can form.^{9,15,18} While it has been speculated that excimers are detrimental to stability,⁹ this connection has not been demonstrated experimentally.

As excimer formation relies on intermolecular interactions, excimers are less likely to form in dilute films. The formation of the excimer in CDBP could therefore be frustrated by diluting with CBP; if the excimer is responsible for the instability of CDBP devices, the lifetime of dilute CDBP devices should approach that of pure CBP devices. To first assess the composition dependence of excimer formation, low-temperature phosphorescence spectroscopy was carried out on films of CDBP in 1,4-bis(triphenylsilyl)benzene (UGH2). UGH2 acts as a transparent matrix for CDBP, permitting changes in phosphorescence to be attributed to changes in excimer formation. Low temperature measurements of phosphorescence have been previously used to identify the CDBP triplet excimer.¹⁸ Figure 3a shows phosphorescence spectra for films of 5, 10, 20, 30, 50 and 100 vol.% CDBP in UGH2. Looking at the most dilute films, the CDBP monomer triplet phosphorescence is defined by two peaks centered at wavelengths of $\lambda = 412$ nm and $\lambda = 440$ nm. In the neat film, triplet excimer emission is characterized by a single broad feature centered at $\lambda = 473$ nm.¹⁵ The CDBP monomer peaks fall in intensity as the concentration is

This is the author's peer reviewed, accepted manuscript. However, the online version of record will be different from this version once it has been copyedited and typeset.

PLEASE CITE THIS ARTICLE AS DOI: 10.1063/1.5124802

increased from 5% to 20% CDBP, with the onset of excimer formation occurring above ~10% CDBP. Figure 3b shows increasingly intense excimer emission is observed above 20% CDBP, with mostly excimer emission observed for CDBP concentrations $\geq 50\%$.

With an understanding of the concentration of CDBP required to form excimers, OLEDs were constructed based on a mixed-host emissive layer of CDBP and CBP. EQE and electrical characteristics for these devices are included in the SM. The peak EQE decreases slightly as CDBP is added to the emissive layer, from 16% for 0% CDBP (100% CBP) to 14% for 100% CDBP devices (Figs. S3-4). Fig. 3b shows the dependence of EL t_{50} lifetime on mixed emissive layer composition for $L_0 = 3000 \text{ cd/m}^2$ (details of voltage rise on PL lifetime in Figs. S5-7). Devices containing $\leq 10\%$ CDBP show nearly identical lifetime behavior to devices containing only CBP. Above the threshold of ~10% CDBP, the lifetime falls sharply. As can be seen in Fig. 3b, the concentration onset of the excimer feature correlates well with the steep reduction in device lifetime, suggesting that the presence of CDBP excimers accelerates degradation in these mixed-host devices. Other potential explanations for the lower stability of CDBP (e.g. if CDBP were chemically less stable or the CDBP source material introduced an impurity) would most likely show a monotonic linear dependence of lifetime on concentration. The distinct concentration threshold behavior observed here makes these alternatives seem unlikely.

To further confirm the role of the triplet excimer state in degradation, optically-pumped degradation was examined for devices containing a phosphorescent ($\text{Ir}(\text{ppy})_3$) or fluorescent (C545T) emitter (Fig. 4). Comparing these emitters allows the effect of host triplets on stability to be isolated. Fluorescent emitters have negligible intersystem crossing; hence, there is negligible generation of triplets under optical pumping of C545T and the host triplet state will not be populated. In contrast, phosphorescent emitters have a large intersystem crossing rate (k_{ISC}) and

This is the author's peer reviewed, accepted manuscript. However, the online version of record will be different from this version once it has been copyedited and typeset.

PLEASE CITE THIS ARTICLE AS DOI: 10.1063/1.5124802

optical pumping will generate a large triplet population which can back transfer to the host triplet state endothermically or exothermically after triplet-triplet annihilation. In the absence of host triplets, the stability of devices containing CBP and CDBP is nearly identical (devices with a C545T emitter in Fig. 4d). In contrast, when host triplets are present, CDBP:Ir(ppy)₃ devices show much lower PL stability under optical pumping than CBP:Ir(ppy)₃ devices (Fig. 4c). Further, when triplets are introduced to the C545T devices *via* electrical pumping, devices with a CDBP host show significantly lower stability than those with CBP, just as was observed with Ir(ppy)₃ (Fig. 4e-f). Combined with Fig. 3, these results strongly support the conclusion that the triplet excimer of CDBP accelerates degradation, as devices are only destabilized when the triplet excimer state is populated.

Given this correlation, there are several theories that could explain the role of the excimer in device degradation. Previous reports have observed an increased excited-state lifetime for excimer triplet states compared to the monomer.⁹ The longer lifetime of excimer states could increase the probability of annihilation events as the exciton density is proportional to lifetime.³⁴ We measured the triplet lifetime of each host by varying the delay time between the laser pulse and spectrum acquisition. The triplet lifetimes of both hosts are within error ($\tau \sim 950$ ms, Fig. S9), invalidating this explanation. However, another possibility is that the triplet diffusivity is higher in CDBP, which would increase the triplet-triplet annihilation rate and accelerate degradation.^{1,35} Further studies should consider if the host triplet diffusivity impacts degradation by measuring the triplet lifetime and triplet diffusion length.³⁶

Alternatively, it is possible that the localization of the excited state is responsible for the observed stability difference. Since the excimer state in CDBP is localized to the end carbazole groups,¹⁵ excess energy given off during relaxation of hot excited states may be concentrated closer

This is the author's peer reviewed, accepted manuscript. However, the online version of record will be different from this version once it has been copyedited and typeset.

PLEASE CITE THIS ARTICLE AS DOI: 10.1063/1.5124802

to the weakest bond (C-N).³⁷ It is also possible that the position of the excimer state allows it to more easily exchange energy with nearby excited states, increasing TTA and accelerating degradation. The more centrally located excited state of CBP, in contrast, may be shielded from neighboring triplets and thus have lower TTA. Given that other carbazole derivatives also exhibit similar excimer formation behavior, the conclusions from this study may apply more generally to other systems.¹⁸ Therefore, this work suggests that additional screening for excimer formation should be considered in OLED host design.

In summary, we study lifetime differences for OLEDs based on two carbazole hosts with similar molecular structures. The appreciable difference in stability for devices based on CDBP and CDP is found to correlate with the formation of host excimer states, highlighting the importance of host molecule triplet states and exciton localization in device degradation. Using LDI-TOF-MS, we show that the lifetime reduction does not correspond with the formation of new fragment molecules. Instead, the presence of excimer states appears to accelerate degradation of CDBP *via* the same C-N bond cleavage which occurs in CBP. These conclusions are confirmed by selectively exciting the triplet state with optically-pumped degradation tests and by frustrating excimer formation by diluting CDBP in CBP. Based on these findings, candidate molecules should be screened for excimer formation early in the design of an OLED stack. This work reinforces the importance of understanding bimolecular interactions in hosts, as they can ultimately drive the degradation of OLEDs.

Supplementary Material

See supplementary material for details on LDI-TOF-MS measurements, additional device efficiency and lifetime characterization, and triplet lifetime characterization of CBP and CDBP.

This is the author's peer reviewed, accepted manuscript. However, the online version of record will be different from this version once it has been copyedited and typeset.

PLEASE CITE THIS ARTICLE AS DOI: 10.1063/1.5124802

Acknowledgements

This work was supported by DuPont Electronics and Imaging. J.S.B. acknowledges support from the National Science Foundation (NSF) Graduate Research Fellowship under Grant No. 00039202. Mass spectrometry was performed at The University of Minnesota (UMN) Department of Chemistry Mass Spectrometry Laboratory (MSL), supported by the Office of the Vice President of Research, College of Science and Engineering, and the Department of Chemistry at UMN, as well as through NSF Grant No. CHE-1336940. The content of this paper is the sole responsibility of the authors and does not represent endorsement by the MSL.

This is the author's peer reviewed, accepted manuscript. However, the online version of record will be different from this version once it has been copyedited and typeset.

PLEASE CITE THIS ARTICLE AS DOI: 10.1063/1.5124802

References

- ¹ S. Scholz, D. Kondakov, B. Lüssem, and K. Leo, *Chemical Reviews* **115**, 8449 (2015).
- ² H. Aziz, *Science* **283**, 1900 (1999).
- ³ H. Sasabe and J. Kido, *Journal of Materials Chemistry C* **1**, 1699 (2013).
- ⁴ C. Adachi, M.A. Baldo, M.E. Thompson, and S.R. Forrest, *Journal of Applied Physics* **90**, 5048 (2001).
- ⁵ D. Wagner, M. Rothmann, P. Strohriegl, C. Lennartz, I. Münster, G. Wagenblast, and C. Schildknecht, in *Organic Light Emitting Materials and Devices XVI* (2012), p. 84761O.
- ⁶ S. Tokito, T. Iijima, Y. Suzuri, H. Kita, T. Tsuzuki, and F. Sato, *Applied Physics Letters* **83**, 569 (2003).
- ⁷ R.J. Holmes, S.R. Forrest, Y.-J. Tung, R.C. Kwong, J.J. Brown, S. Garon, and M.E. Thompson, *Applied Physics Letters* **82**, 2422 (2003).
- ⁸ A. Chaskar, H.F. Chen, and K.T. Wong, *Advanced Materials* **23**, 3876 (2011).
- ⁹ S.T. Hoffmann, P. Schrögel, M. Rothmann, R.Q. Albuquerque, P. Strohriegl, and A. Köhler, *Journal of Physical Chemistry B* **115**, 414 (2011).
- ¹⁰ A. Ya Freidzon, A.A. Safonov, A.A. Bagaturyants, D.N. Krasikov, B. V Potapkin, A.A. Osipov, A. V Yakubovich, and O. Kwon, (2017).
- ¹¹ Q. Wang, B. Sun, and H. Aziz, *Advanced Functional Materials* **24**, 2975 (2014).
- ¹² H. Yu, Y. Zhang, Y.J. Cho, and H. Aziz, *ACS Applied Materials & Interfaces* **9**, 14145 (2017).
- ¹³ Q. Wang, B. Sun, and H. Aziz, *Advanced Functional Materials* **24**, 2975 (2014).
- ¹⁴ T. Setzer, P. Friederich, V. Meded, W. Wenzel, C. Lennartz, and A. Dreuw, *ChemPhysChem* **19**, 2961 (2018).
- ¹⁵ S.A. Bagnich, S. Athanasopoulos, A. Rudnick, P. Schroegel, I. Bauer, N.C. Greenham, P. Strohriegl, and A. Kö, (2015).
- ¹⁶ D.F. O'Brien, M.A. Baldo, M.E. Thompson, and S.R. Forrest, *Applied Physics Letters* **74**, 442 (1999).
- ¹⁷ M.A. Baldo, S. Lamansky, P.E. Burrows, M.E. Thompson, and S.R. Forrest, *Applied Physics Letters* **75**, 4 (1999).
- ¹⁸ S.A. Bagnich, A. Rudnick, P. Schroegel, P. Strohriegl, and A. Köhler, *Philosophical Transactions of the Royal Society A: Mathematical, Physical and Engineering Sciences* **373**, 20140446 (2015).
- ¹⁹ R. Seifert, I. Rabelo de Moraes, S. Scholz, M.C. Gather, B. Lüssem, and K. Leo, *Organic Electronics* **14**, 115 (2013).

This is the author's peer reviewed, accepted manuscript. However, the online version of record will be different from this version once it has been copyedited and typeset.

PLEASE CITE THIS ARTICLE AS DOI: 10.1063/1.5124802

- ²⁰ S. Schmidbauer, A. Hohenleutner, and B. König, *Advanced Materials* **25**, 2114 (2013).
- ²¹ S. Scholz, K. Walzer, and K. Leo, *Advanced Functional Materials* **18**, 2541 (2008).
- ²² C. Jeong, C. Coburn, M. Idris, Y. Li, P.I. Djurovich, M.E. Thompson, and S.R. Forrest, *Organic Electronics: Physics, Materials, Applications* **64**, 15 (2019).
- ²³ J.S. Bangsund, K.W. Hershey, and R.J. Holmes, *ACS Applied Materials & Interfaces* **10**, 5693 (2018).
- ²⁴ K.W. Hershey, J. Suddard-Bangsund, G. Qian, and R.J. Holmes, *Applied Physics Letters* **111**, 113301 (2017).
- ²⁵ J.S. Bangsund, K.W. Hershey, D.C.K. Rathwell, H.Y. Na, J.H. Jeon, P. Trefonas, and R.J. Holmes, *Journal of the Society for Information Display* jsid. 761 (2019).
- ²⁶ J. Sohn, D. Ko, H. Lee, J. Han, S.D. Lee, and C. Lee, *Organic Electronics: Physics, Materials, Applications* **70**, 286 (2019).
- ²⁷ R. Meerheim, K. Walzer, M. Pfeiffer, and K. Leo, *Applied Physics Letters* **89**, 061111 (2006).
- ²⁸ W. Song and J.Y. Lee, *Advanced Optical Materials* **5**, 1600901 (2017).
- ²⁹ D. Jacquemin and D. Escudero, *Chemical Science* **8**, 7844 (2017).
- ³⁰ D.Y. Kondakov, W.C. Lenhart, and W.F. Nichols, *Journal of Applied Physics* **101**, 024512 (2007).
- ³¹ S. Schmidbauer, A. Hohenleutner, and B. König, *Advanced Materials* **25**, 2114 (2013).
- ³² R. Seifert, I. Rabelo De Moraes, S. Scholz, M.C. Gather, B. Lüssem, and K. Leo, (2013).
- ³³ I.R. de Moraes, S. Scholz, B. Lüssem, and K. Leo, *Organic Electronics* **12**, 341 (2011).
- ³⁴ S. Reineke, G. Schwartz, K. Walzer, and K. Leo, *Physica Status Solidi (RRL) - Rapid Research Letters* **3**, 67 (2009).
- ³⁵ S. Reineke, G. Schwartz, K. Walzer, M. Falke, and K. Leo, *Appl. Phys. Lett.* **94**, 163305 (2009).
- ³⁶ D. Rai and R. J. Holmes, *Journal of Materials Chemistry C* **7**, 5695 (2019).
- ³⁷ J. Lee, C. Jeong, T. Batagoda, C. Coburn, M.E. Thompson, and S.R. Forrest, *Nat Commun* **8**, (2017).

This is the author's peer reviewed, accepted manuscript. However, the online version of record will be different from this version once it has been copyedited and typeset.

PLEASE CITE THIS ARTICLE AS DOI: 10.1063/1.5124802

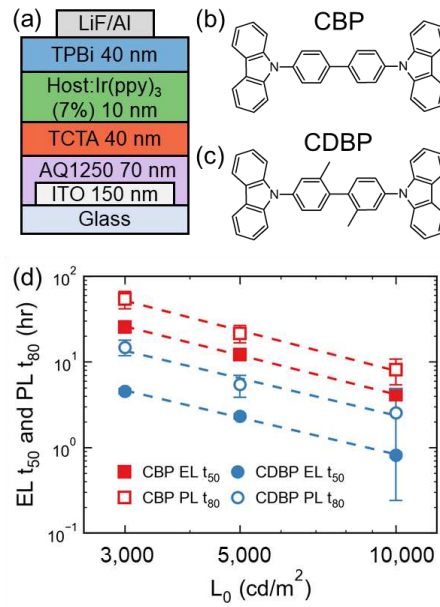


Figure 1: (a) Device architecture used in this study. (b)-(c) Molecular structures of (b) CBP and (c) CDBP. (d) EL t₅₀ and photoluminescence (PL) t₈₀ as a function of initial luminance for devices based on each host.

This is the author's peer reviewed, accepted manuscript. However, the online version of record will be different from this version once it has been copyedited and typeset.

PLEASE CITE THIS ARTICLE AS DOI: 10.1063/1.5124802

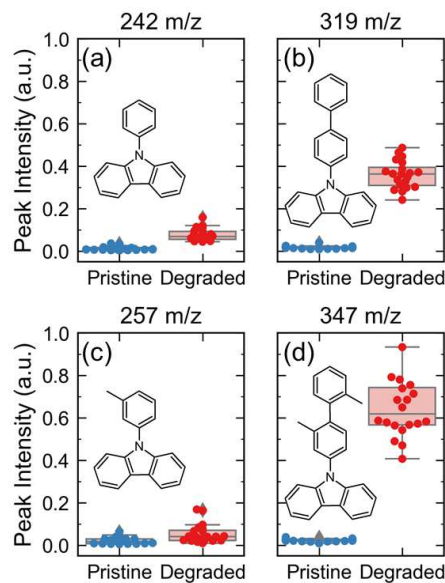


Figure 2: LDI-TOF MS data for CBP and CDBP devices. (a)-(b) Show integrated peak intensities of pristine and degraded CBP devices for fragments with masses of (a) 242 amu and (b) 319 amu. (c)-(d) Show integrated peak intensities of CDBP devices for fragments with masses of (c) 257 amu and (d) 347 amu.

This is the author's peer reviewed, accepted manuscript. However, the online version of record will be different from this version once it has been copyedited and typeset.

PLEASE CITE THIS ARTICLE AS DOI: 10.1063/1.5124802

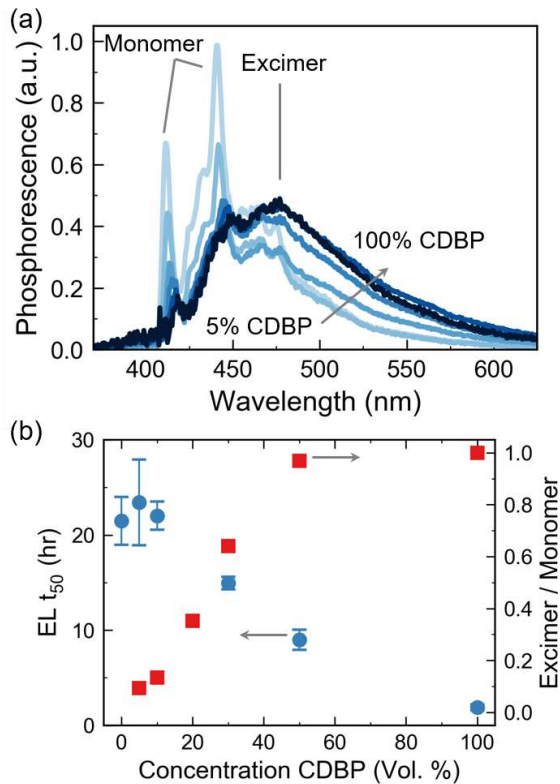


Figure 3: (a) Low temperature phosphorescence spectra of thin films of CDBP doped in UGH2 as a function of concentration. (b) EL t_{50} at an initial luminance of 3,000 cd/m^2 of CBP:CDBP mixed host devices as a function of CDBP concentration (blue circles). Excimer to monomer signal ratio extracted from the phosphorescence intensity in (a) at wavelengths of $\lambda = 525\text{nm}$ and $\lambda = 412\text{ nm}$ (red squares). The onset of excimer signal $>10\%$ CDBP corresponds well with the decrease in lifetime.

This is the author's peer reviewed, accepted manuscript. However, the online version of record will be different from this version once it has been copyedited and typeset.

PLEASE CITE THIS ARTICLE AS DOI: 10.1063/1.5124802

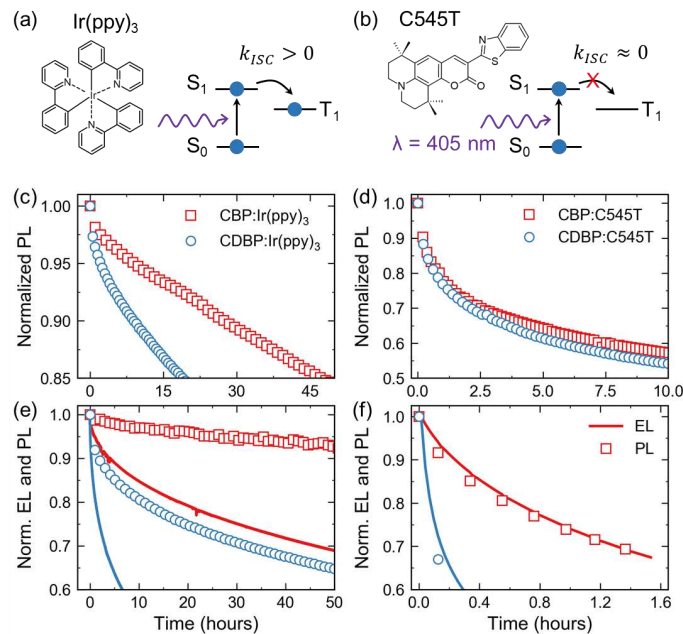
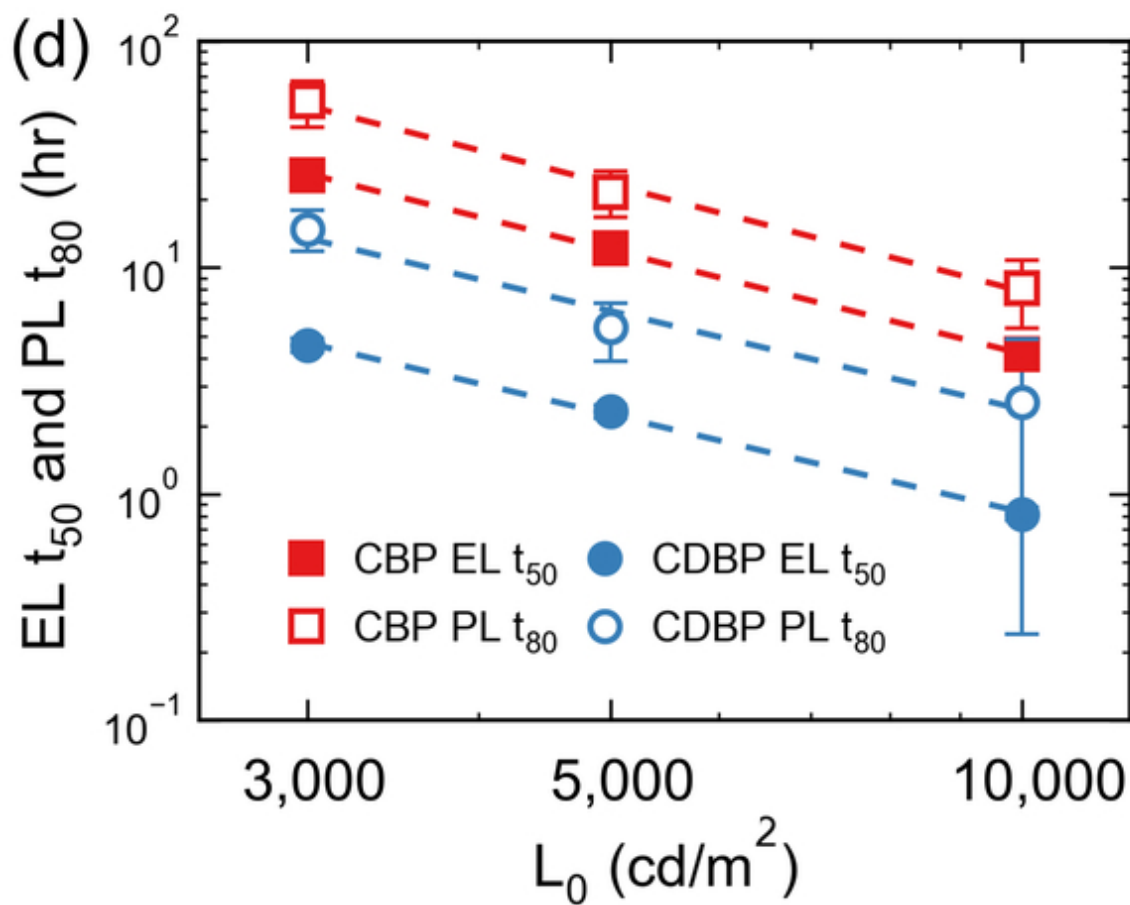
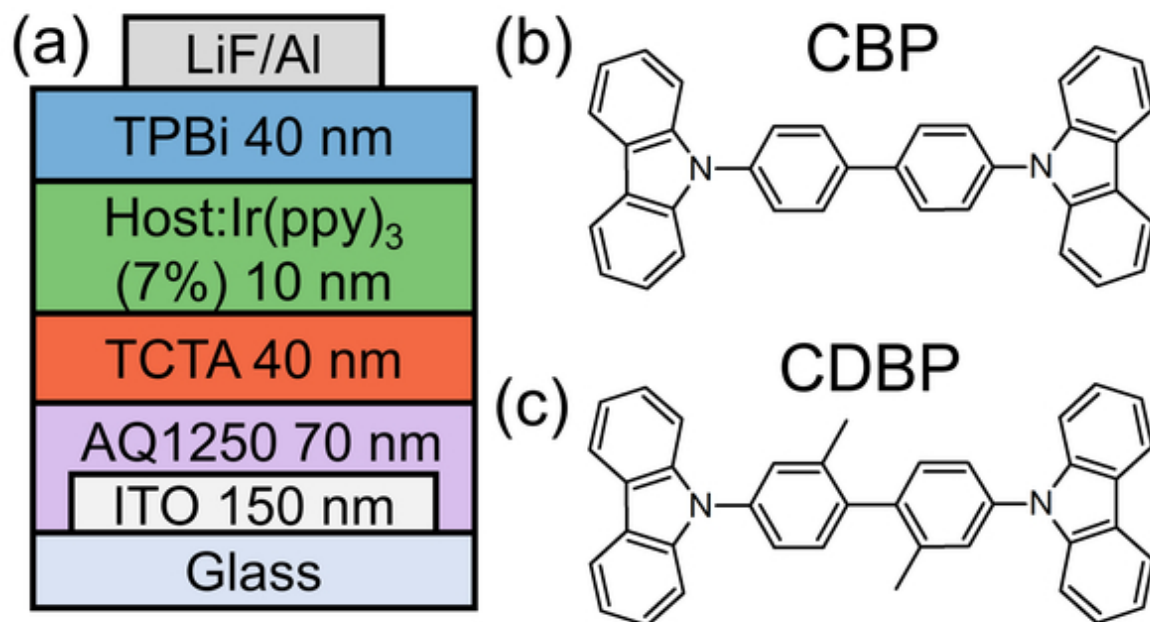


Figure 4: (a) Molecular structure of the phosphorescent emitter, Ir(ppy)₃, and schematic showing that triplets are generated during optical pumping due to non-zero intersystem crossing. (b) Molecular structure of the fluorescent emitter, C545T, and schematic showing that negligible triplet formation occurs during optical pumping due to vanishing intersystem crossing. Normalized PL decays during optically-pumped degradation ($\lambda = 405$ nm) of devices with (c) Ir(ppy)₃ and (d) C545T doped in each host. Normalized EL and PL decays during electrically-pumped degradation of devices with (e) Ir(ppy)₃ and (f) C545T doped in each host. Ir(ppy)₃ devices were degraded at $L_0 = 1,000$ cd/m² and C545T devices were degraded at $L_0 = 500$ cd/m². For optical degradation of C545T in (d), the pump fluence during degradation was $\sim 10,000$ mW/cm² and a servo-mounted neutral density filter was used to attenuate the beam to $\sim 1,000$ mW/cm² during the PL measurement to limit bimolecular quenching.

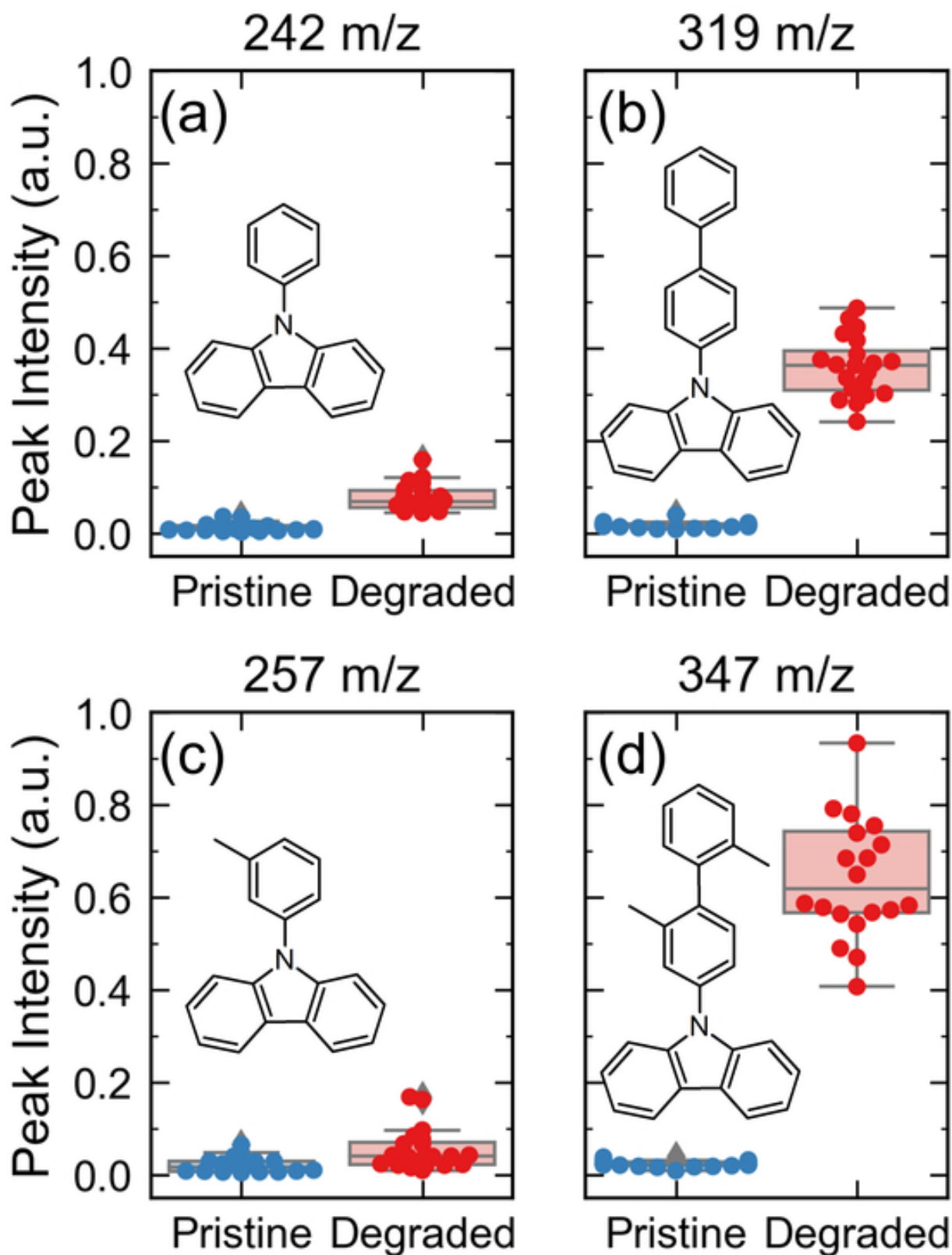
This is the author's peer reviewed, accepted manuscript. However, the online version of record will be different from this version once it has been copyedited and typeset.

PLEASE CITE THIS ARTICLE AS DOI: 10.1063/1.5124802



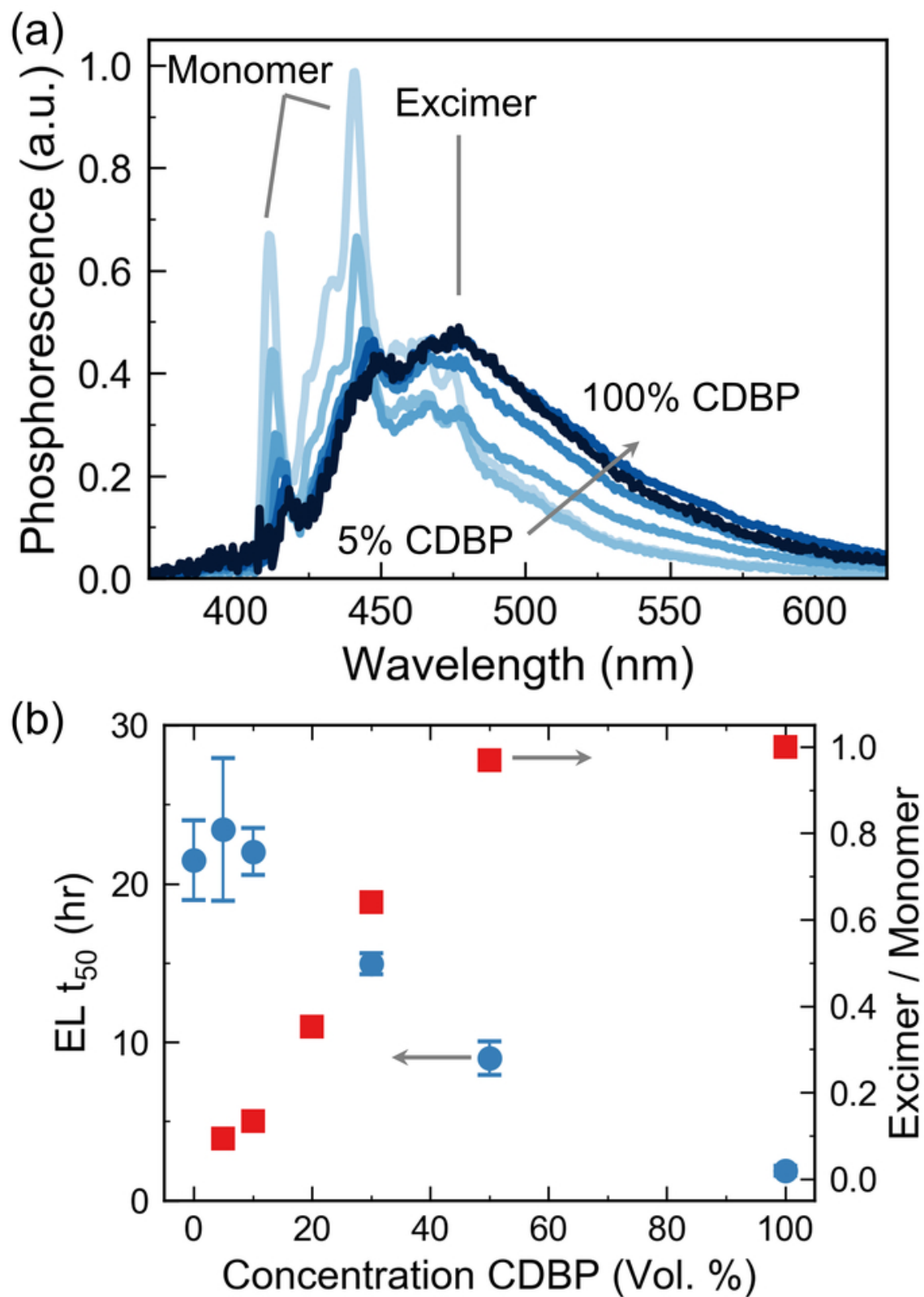
This is the author's peer reviewed, accepted manuscript. However, the online version of record will be different from this version once it has been copyedited and typeset.

PLEASE CITE THIS ARTICLE AS DOI: 10.1063/1.5124802



This is the author's peer reviewed, accepted manuscript. However, the online version of record will be different from this version once it has been copyedited and typeset.

PLEASE CITE THIS ARTICLE AS DOI: 10.1063/1.5124802



This is the author's peer reviewed, accepted manuscript. However, the online version of record will be different from this version once it has been copyedited and typeset.

PLEASE CITE THIS ARTICLE AS DOI: 10.1063/1.5124802

